Journal of Porphyrins and Phthalocyanines
J. Porphyrins Phthalocyanines 2019; **23**: 213–222
DOI: 10.1142/S1088424619500214

Published at http://www.worldscinet.com/jpp/

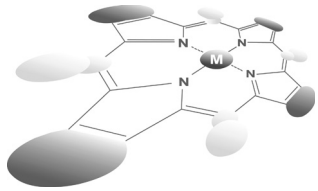

Synthesis, electrochemistry, protonation and X-ray analysis of *meso*-aryl substituted open-chain pentapyrroles

Wenqian Shan[a], Valentin Quesneau[b], Nicolas Desbois[b], Virginie Blondeau-Patissier[c], Mario L. Naitana[b], Yoann Rousselin[b], Claude P. Gros*[b◊], Zhongping Ou[a◊] and Karl M. Kadish*[a◊]

[a]*University of Houston, Department of Chemistry, Houston, Texas, 77204-5003, USA*
[b]*Université de Bourgogne Franche-Comté, ICMUB (UMR UB-CNRS 6302), 9 Avenue Alain Savary, BP 47870, 21078 Dijon Cedex, France*
[c]*Université de Bourgogne Franche-Comté, Institut FEMTO-ST, UMR CNRS 6174, Department Time-Frequency, 26 Chemin de l'épitaphe, 25030 Besançon Cedex, France*

This paper is part of the 2019 Women in Porphyrin Science special issue.

Received 26 December 2018
Accepted 31 January 2019

ABSTRACT: Five *meso*-tetraaryl open-chain pentapyrroles were synthesized and characterized as to their electrochemistry and protonation reactions in nonaqueous media. The investigated compounds are represented as $(Ar)_4PPyH_3$ where Ar = *m*,*m*-F_2Ph, *p*-BrPh, Ph, *m*,*p*,*m*-$(OMe)_3$Ph or *p*-MePh and were characterized by UV-vis and ^{1}H NMR spectroscopy, mass spectrometry and electrochemistry. Cyclic voltammetry was used to measure redox potentials, while protonation involving the conversion of $(Ar)_4PPyH_3$ to $[(Ar)_4PPyH_5]^{2+}$ was monitored by UV-vis absorption spectroscopy. Equilibrium constants for proton addition were calculated using the Hill equation. One of the pentapyrroles was also structurally characterized. The electrochemical data, protonation constants and crystal structure were then compared with data for previously examined pentapyrroles and analyzed as a function of the solvent properties and nature of substituents on the *meso*-phenyl rings of the macrocycle.

KEYWORDS: open-chain pentapyrrole, synthesis, electrochemistry, protonation reactions, X-ray analysis.

INTRODUCTION

Open-chain pentapyrroles (or pentapyrrotetramethenes) with *meso*-tetraaryl substituents were first isolated as a major side product in the synthesis of corroles, being obtained in high yield (11%, the same as the target product) [1], and these molecules have since attracted great attention as synthetic precursors for the related sapphyrin macrocycles [1–8].

Our own interest in open-chain pentapyrroles has involved a characterization of their electrochemistry, spectroelectrochemistry and acid-base properties in nonaqueous media, as well as a study of their conversion to the corresponding sapphyrins [5–8]. The open-chain pentapyrroles were shown to undergo two reversible one-electron reductions in CH_2Cl_2, PhCN or pyridine, with the $E_{1/2}$ values for these processes varying only slightly with the utilized electrochemical solvent [5, 6]. However, in contrast to the well-defined reductions of open-chain pentapyrroles, the oxidation behavior of these compounds was shown to vary as a function of the selected solvent. Cations and dications of the pentapyrroles could be generated and characterized prior to sapphyrin formation in CH_2Cl_2 or PhCN [5] but this was not the case in pyridine where deprotonation was proposed to occur after

◊ SPP full member in good standing.

*Correspondence to: Claude P. Gros, tel.: (33) 03 80 39 61 12, fax: (33) 03 80 39 61 17, email: Claude.Gros@u-bourgogne.fr; Karl M. Kadish, tel.: (1) 713-743-2740, fax: (1) 713-743-2745, email: kkadish@uh.edu.

the abstraction of one electron in the basic solvent [6]. Additional oxidation processes were also observed in the cyclic voltammograms of pentapyrroles with sterically hindered or highly electron-withdrawing groups, and it was suggested [5, 8] that this might be related to the products formed in a proton-induced conversion to the corresponding sapphyrins.

The acid-base properties of several open-chain pentapyrroles were previously examined in our laboratory and the equilibrium constants for proton addition to these compounds were determined utilizing spectroscopic monitoring of the reaction. Two protons could be easily added to the open-chain pentapyrroles with the measured $\log\beta_2$ for this reaction ranging from 8.1 to 11.0 [5, 8]. Two protons could also be abstracted with $\log\beta_2$ values ranging from 5.1 to 6.4 [6]. Detailed studies of the proton-induced conversion of pentapyrroles to the corresponding sapphyrins are described in the literature [7, 8].

In the present paper, a new series of open-chain pentapyrroles containing different *meso*-aryl groups were synthesized and characterized as to their spectral and electrochemical properties in CH_2Cl_2, PhCN and pyridine (Py). Their protonation reactions were also investigated. A single-crystal analysis of one compound is given in the present study and comparisons are made with an earlier reported open-chain pentapyrrole structure. The five newly investigated compounds are shown in Chart 1 and are represented as $(Ar)_4PPyH_3$ where Ar = *m*,*m*-F_2Ph **1**, *p*-BrPh **2**, Ph **3**, *m*,*p*,*m*-$(OMe)_3$Ph **4** or *p*-MePh **5**.

EXPERIMENTAL

Chemicals

All chemicals and solvents were of analytical grade. Silica gel 60 (70–230 and 230–400 mesh, Sigma-Aldrich) was used for column chromatography. Absolute dichloromethane (CH_2Cl_2, 99.8%) from EMD Chemicals Inc. and pyridine (Py, HPLC) from Sigma-Aldrich Chemical Co. were used for electrochemistry without further purification. Benzonitrile (PhCN, 99%) was purchased from Sigma-Aldrich Chemical Co. and distilled over P_2O_5 under vacuum prior to use. Tetra-*n*-butylammonium perchlorate (TBAP) was purchased from Sigma-Aldrich and used as supporting electrolyte without further purification.

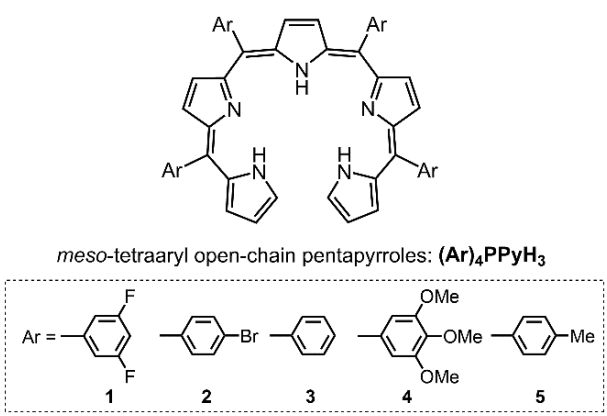

Chart 1. Structures of investigated compounds **1–5**

Instrumentation

^{1}H NMR spectra were recorded with Bruker AV300, AV400 or AV500 spectrometers (300, 400 and 500 MHz, respectively) and $CDCl_3$ was used as a solvent in each case except when otherwise indicated. Chemical shifts (δ) in the ^{1}H NMR spectra are given in ppm and are relative to residual $CHCl_3$ (7.26 ppm). MALDI/TOF mass spectra were recorded on a Bruker Ultraflex Extreme MALDI Tandem TOF Mass Spectrometer.

Cyclic voltammetry was carried out with an EG&G model 173 potentiostat/galvanostat with a homemade cell and a three-electrode system which consisted of a glassy carbon working electrode (diameter = 3 mm), a platinum wire counter electrode and a saturated calomel reference electrode (SCE). The SCE was separated from the bulk of the solution by a fritted-glass bridge of low porosity which contained the solvent/supporting electrolyte mixture.

Calculation of protonation constants

Equilibrium constants for the addition of protons to the neutral pentapyrroles were determined by monitoring the spectral changes in CH_2Cl_2 during titrations of the compounds with trifluoroacetic acid (TFA) in CH_2Cl_2. The acid titration reagents were prepared in CH_2Cl_2 with different concentrations of TFA. Ten to one hundred microliters of reagent were gradually added to a 4.0 mL stock solution (about 10^{-5} M) of the investigated compounds in CH_2Cl_2 and changes in the UV-vis spectra during the titration were analyzed as a function of the concentration of added acid. Equilibrium constants were calculated using the Hill equation [9].

Synthesis

The investigated open-chain pentapyrroles were synthesized from the corresponding aryl-aldehyde (20 mmol, 1 eq.) and pyrrole (40 mmol, 2 eq.) according to a previously published method [5, 8]. Purification and characterization details for each compound are described below.

(*m*,*m*-F_2Ph)$_4$PPyH$_3$ 1 was obtained in 5.3% yield (114 mg, 0.138 mmol). The crude product was chromatographed on basic alumina with CH_2Cl_2/heptane (1/2, v/v) to 100% of CH_2Cl_2 then on silica gel with CH_2Cl_2/heptane (1/1, v/v) and on silica gel with toluene/pentane (1/1, v/v). ^{1}H NMR (500 MHz, $CDCl_3$) δ (ppm): 12.60 (s, 3H, NH), 7.00 (m, 4H, Ph), 6.90–6.79 (m, 8H, Ph), 6.73 (s, 2H, H-pyrrolic), 6.58 (d, *J* = 4.5 Hz, 2H,

H-pyrrolic), 6.52 (m, 2H, H-pyrrolic), 6.44 (m, J = 4.5 Hz, 2H, H-pyrrolic), 6.10 (m, 2H, H-pyrrolic), 6.06 (m, 2H, H-pyrrolic). MS (MALDI/TOF): *m/z* 826.02 $[M + H]^+$, 826.22 calcd for $C_{48}H_{28}F_8N_5$. HR-MS (MALDI/TOF): *m/z* 825.2122 $[M]^{+\bullet}$, 825.2133 calcd for $C_{48}H_{27}F_8N_5$.

(*p*-BrPh)$_4$PPyH$_3$ 2 was obtained in 2.3% yield (112 mg, 0.112 mmol). The crude product was chromatographed on a short plug of silica gel with dichloromethane as eluent. The second red fraction containing the desired open-chain pentapyrrole **2** was passed through a second plug of silica with a mixture of CH_2Cl_2/heptane (6/4, v/v) and recrystallized in a mixture of CH_2Cl_2 and MeOH. ^{1}H NMR (300 MHz, $CDCl_3$) δ (ppm): 12.68 (br s, 3H, NH), 7.57 (d, J = 9.0 Hz, 4H, Ph), 7.46 (d, J = 9.0 Hz, 4H, Ph), 7.33 (d, J = 8.5 Hz, 4H, Ph), 7.09 (d, J = 8.5 Hz, 4H, Ph), 6.66 (s, 2H, H-pyrrolic), 6.56 (d, J = 4.5 Hz, 2H, H-pyrrolic), 6.48 (m, 4H, H-pyrrolic), 6.40 (d, J = 5.0 Hz, 2H, H-pyrrolic), 6.02 (d, J = 4.0 Hz, 2H, H-pyrrolic), 5.96 (d, J = 4.0 Hz, 2H). MS (MALDI/TOF): *m/z* 992.87 $[M]^{+\bullet}$, 992.93 calcd for $C_{48}H_{31}Br_4N_5$. HR-MS (MALDI/TOF): *m/z* 993.9421 $[M + H]^+$, 993.9386 calcd for $C_{48}H_{32}Br_4N_5$.

(Ph)$_4$PPyH$_3$ 3 was obtained in 1.5% yield (53 mg, 0.078 mmol). The crude product was chromatographed on silica with a mixture of CH_2Cl_2 and heptane (2/1, v/v). The second red fraction containing the desired open-chain pentapyrrole **3** was passed through a second plug of silica with a mixture of CH_2Cl_2/heptane (2/1, v/v) and recrystallized in a mixture of CH_2Cl_2 and MeOH. ^{1}H NMR (400 MHz, CD_3COOCD_3) δ (ppm): 12.91 (br s, 3H, NH), 7.50 (d, J = 4.5 Hz, 8H, Ph), 7.45–7.35 (m, 8H, Ph), 7.29–7.27 (m, 4H, Ph), 6.68 (s, 2H, H-pyrrolic), 6.61 (s, 2H, H-pyrrolic), 6.56 (d, J = 4.5 Hz, 2H, H-pyrrolic), 6.42 (d, J = 4.5 Hz, 2H, H-pyrrolic), 6.03 (s, 4H, H-pyrrolic). MS (MALDI/TOF): *m/z* 682.90 $[M+H]^+$, 682.30 calcd for $C_{48}H_{35}N_5$.

(*m,p,m*-(OMe)$_3$Ph)$_4$PPyH$_3$ 4 was obtained in 8.8% yield (460 mg, 0.479 mmol) [4]. The crude product was chromatographed on a short plug of silica gel with 2% THF in CH_2Cl_2 as eluent. The second red fraction was collected and recrystallized in a mixture of THF and ethanol (1:1) to afford a red/green solid. ^{1}H NMR (600 MHz, $CDCl_3$) δ (ppm): 12.62 (br s, 3H), 6.82 (s, 2H, H-pyrrolic), 6.73 (m, 6H, Ph, H-pyrrolic), 6.63–6.45 (m, 6H, Ph, H-pyrrolic), 6.43 (s, 2H, H-pyrrolic), 6.15 (d, J = 3.7 Hz, 2H, H-pyrrolic), 5.95 (m, 2H, H-pyrrolic), 3.95 (s, 6H, OCH_3), 3.90 (m, 18H, OCH_3), 3.81 (s, 12H, OCH_3). MS (MALDI/TOF): *m/z* 1042.37 $[M + H]^+$, 1042.42 calcd for $C_{60}H_{60}N_5O_{12}$.

(*p*-MePh)$_4$PPyH$_3$ 5 was obtained in 3.3% yield (121.8 mg, 0.166 mmol). The crude product was chromatographed on silica with a mixture of CH_2Cl_2 and heptane (4/6, v/v) and 100% of CH_2Cl_2. ^{1}H NMR (300 MHz, $CDCl_3$) δ (ppm): 12.82 (s, 3H, NH), 7.35 (d, J = 8.0 Hz, 4H, Ph), 7.23 (d, J = 8.0 Hz, 4H, Ph), 7.12 (m, 8H, Ph), 6.64 (s, 2H, H-pyrrolic), 6.59 (d, J = 4.5 Hz, 2H, H-pyrrolic), 6.50 (m, 2H, H-pyrrolic), 6.42 (d, J = 4.5 Hz, 2H, H-pyrrolic), 6.04 (m, 2H, H-pyrrolic), 5.94 (m, 2H, H-pyrrolic), 2.43 (s, 6H, CH_3), 2.39 (s, 6H, CH_3). MS (MALDI/TOF): *m/z* 738.29 $[M+H]^+$, 738.36 calcd for $C_{52}H_{44}N_5$. HR-MS (MALDI/TOF): *m/z* 737.3515 $[M]^{+\bullet}$, 737.3513 calcd for $C_{52}H_{43}N_5$.

Single crystal X-ray analysis and crystal data

Single clear dark violet plate-shaped crystals of compound **2** were recrystallized from a mixture of chloroform and methanol by slow evaporation. A suitable crystal (0.36 × 0.21 × 0.17) mm^3 was selected and mounted on a MITIGEN holder oil on a Bruker D8 VENTURE (Cu) diffractometer. The crystal was kept at T = 100 (1) K during data collection. Using **Olex2**, [10] the structure was solved with the **ShelXT** structure solution program [11] using the Intrinsic Phasing solution method. The model was refined with version 2016/6 of ShelXL using Least Squares minimization.

$C_{49}H_{32}Br_4Cl_3N_5$, M_r = 1116.78, orthorhombic, P*bcn* (No. 60), a = 25.9378 (13) Å, b = 14.7363 (7) Å, c = 23.1798 (11) Å, V = 8859.9 (7) Å^3, T = 100 (1) K, Z = 8, Z' = 1, μ(CuK_α) = 6.430, 49093 reflections measured, 7853 unique (R_{int} = 0.0541) which were used in all calculations. The final wR_2 was 0.0853 (all data) and R_1 was 0.0359 ($I > 2\sigma(I)$). CCDC-1554869 contains the supplementary crystallographic data for this paper. These data can be obtained free of charge from The Cambridge Crystallographic Data Centre *via* www.ccdc.cam.ac.uk/data_request/cif.

RESULTS AND DISCUSSION

Synthesis and characterization

The five open-chain pentapyrroles in Chart 1 were isolated as side products in the synthesis of structurally related triarylcorroles according to methods described in the literature [5, 8]. The newly synthesized compounds were then fully characterized by ^{1}H NMR spectroscopy, mass spectrometry (MS MALDI/TOF) and high-resolution mass spectrometry (HRMS MALDI/TOF). The molecular weights of the compounds were determined by mass spectrometry and show, in each case, a perfect match with the calculated molar mass. Characteristic chemical shift data in the ^{1}H NMR spectra also confirmed the target compounds **1–5** to have the structures shown in Chart 1.

Absorption spectra of the compounds **1–5** were measured at a concentration of 10^{-3} M in CH_2Cl_2, PhCN and pyridine containing 0.1 M TBAP (Fig. S11 and Table S1). Two or three intense bands (ε = ~10^4 cm^{-1}·M^{-1}) were present in the Soret region of the spectrum while one or two broad bands of lower intensity (ε = ~10^3 cm^{-1}·M^{-1}) are seen in the visible region.

The above spectroscopic properties are all consistent with previously reported spectral data for similar

compounds [5, 7, 8]. Additional detailed information on the synthesis and characterization are given in supporting information (Figs S1–S11) and in the Experimental section.

Electrochemistry

The electrochemistry of compounds **1–5** was characterized by cyclic voltammetry in CH_2Cl_2, PhCN or pyridine containing 0.1 M TBAP. Examples of cyclic voltammograms for compound **4** in those three solvents containing 0.1 M TBAP are given in Fig. 1 and a summary of the measured half-wave potentials for reductions and oxidations in each solvent are given in Table 1.

As shown in Fig. 1, two reversible reductions occur in each solvent. Two reversible oxidations are also seen in CH_2Cl_2 and PhCN, but this is not the case in pyridine which reacts with the singly oxidized pentapyrrole as previously described [6]. Regardless of the solvent, two electrons can be abstracted from the conjugated π-system of the pentapyrrole under the given solution conditions.

The separation in $E_{1/2}$ between the two one-electron oxidations in CH_2Cl_2 or PhCN (0.22 V) are smaller than the separation in pyridine (0.30 V) as seen in Fig. 1. Moreover, the electrochemical HOMO–LUMO gap (the potential difference between the first oxidation and first reduction) decreases upon going from CH_2Cl_2 to PhCN and then to pyridine. For example, in the case of compound **4** (Fig. 1), the electrochemically measured HOMO–LUMO gap is 1.32 eV in CH_2Cl_2, 1.25 eV in PhCN and 1.13 eV in pyridine.

Cyclic voltammograms for all five pentapyrroles in each solvent containing 0.1 M TBAP are given in Figs 2 (in DCM), S12 (in PhCN) and S13 (in pyridine). As shown in Fig. 2, the redox potentials are negatively shifted upon going from compound **1** (which has two electron-withdrawing F atoms on the *meso*-phenyl rings) to compound **5**, which possesses *p*-Me electron-donating groups on the *meso*-phenyl rings. The HOMO–LUMO gap in CH_2Cl_2 averages 1.32 ± 0.04 V while the average gap in the other two solvents, PhCN and pyridine is 1.24 and 1.09 V, respectively (Table 2).

The measured $E_{1/2}$ values for each redox reaction of the open-chain pentapyrroles can be related to the specific electron-donating or electron-withdrawing substituent on the four phenyl rings of the compounds by linear free energy relationships [5, 8]. The relevant correlation is given in equation 1, where ρ is the slope of the of $E_{1/2}$ *vs.* Σσ plot [12] and the values of σ are taken from the literature [12, 13]. The larger the value of ρ (given in volts), the larger is the effect of the electron-donating or electron-withdrawing substituents on the measured half-wave potentials for a given electron transfer reaction, in this case the two one-electron reductions and two one-electron oxidations of the pentapyrroles.

$$\Delta E_{1/2} = \Sigma\sigma\rho \quad (1)$$

Examples of linear free energy relationships for the pentapyrroles in the three electrochemical solvents are given in Figs 3, S11 and S12 where the redox potentials in the plots are listed in Table 1 for the newly investigated compounds and in Table S1 for previously characterized pentapyrroles with different *meso*-phenyl substituents

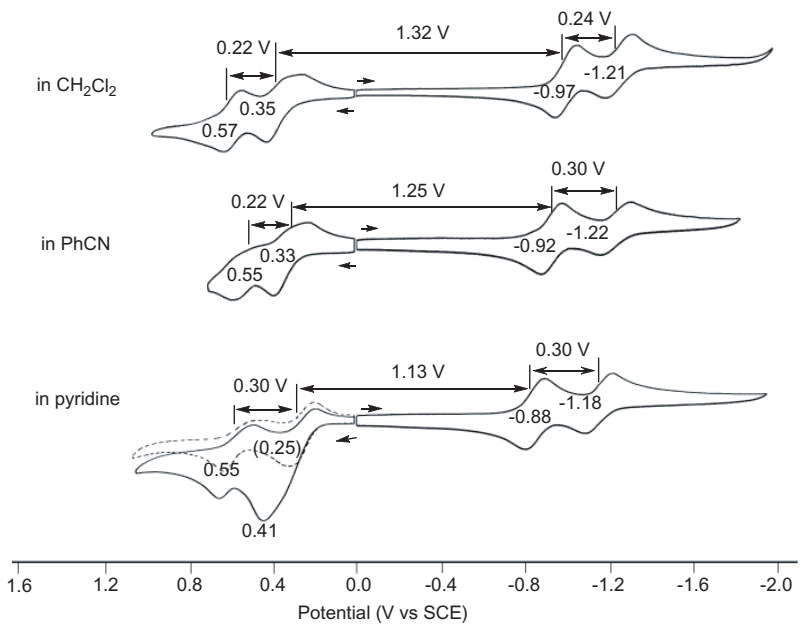

Fig. 1. Cyclic voltammograms of (*m,p,m*-$(OMe)_3Ph)_4PPyH_3$ **4** in CH_2Cl_2, PhCN and pyridine containing 0.1 M TBAP. All current–voltage curves were obtained on the first potential scan except for the oxidation in pyridine which shows the first (solid line) and second (dashed line) potential scans

Table 1. Half-wave potentials (V *vs.* SCE) of $(Ar)_4PPyH_3$ derivatives **1–5** in CH_2Cl_2, PhCN and pyridine containing 0.1 M TBAP

Solvent	X (Ar = XPh)	Σσ[a]	Ox_2	Ox_1	ΔE_{ox}	Red1	Red2	ΔE_{red}	H-L(eV)[b]
CH_2Cl_2	*m,m*-F_2 **1**	2.72	0.77	0.57	0.20	-0.79	-1.05	0.26	1.36
	p-Br **2**	0.92	0.72	0.46	0.16	-0.88	-1.12	0.24	1.34
	H **3**	0.0	0.58	0.33	0.25	-0.98	-1.16	0.18	1.31
	m,p,m-$(OMe)_3$ **4**	-0.12	0.57	0.35	0.22	-0.97	-1.21	0.24	1.32
	p-Me **5**	-0.68	0.49	0.31	0.18	-0.99	-1.20	0.21	1.30
PhCN	*m,m*-F_2 **1**	2.72	0.77	0.56	0.21	-0.69	-0.99	0.30	1.25
	p-Br **2**	0.92	0.60	0.42	0.18	-0.83	-1.12	0.29	1.25
	H **3**	0.0	0.60	0.35	0.25	-0.89	-1.19	0.30	1.24
	m,p,m-$(OMe)_3$ **4**	-0.12	0.55	0.33	0.22	-0.92	-1.22	0.30	1.25
	p-Me **5**	-0.68	0.51	0.29	0.22	-0.94	-1.21	0.27	1.23
pyridine	*m,m*-F_2 **1**	2.72	0.73	0.42	0.31	-0.70	-1.00	0.30	1.12
	p-Br **2**	0.92	0.65	0.30	0.35	-0.78	-1.07	0.29	1.08
	H **3**	0.0	0.60	0.24	0.36	-0.85	-1.12	0.27	1.09
	m,p,m-$(OMe)_3$ **4**	-0.12	0.55	0.25	0.30	-0.88	-1.18	0.30	1.13
	p-Me **5**	-0.68	0.56	0.21[c]	0.35	-0.90	-1.13	0.23	1.11

[a]Values of σ were taken from Ref. [12]. [b]The HOMO–LUMO gap (potential difference between the first oxidation and first reduction). [c]Half-wave potentials for the first oxidation were obtained from the second scan.

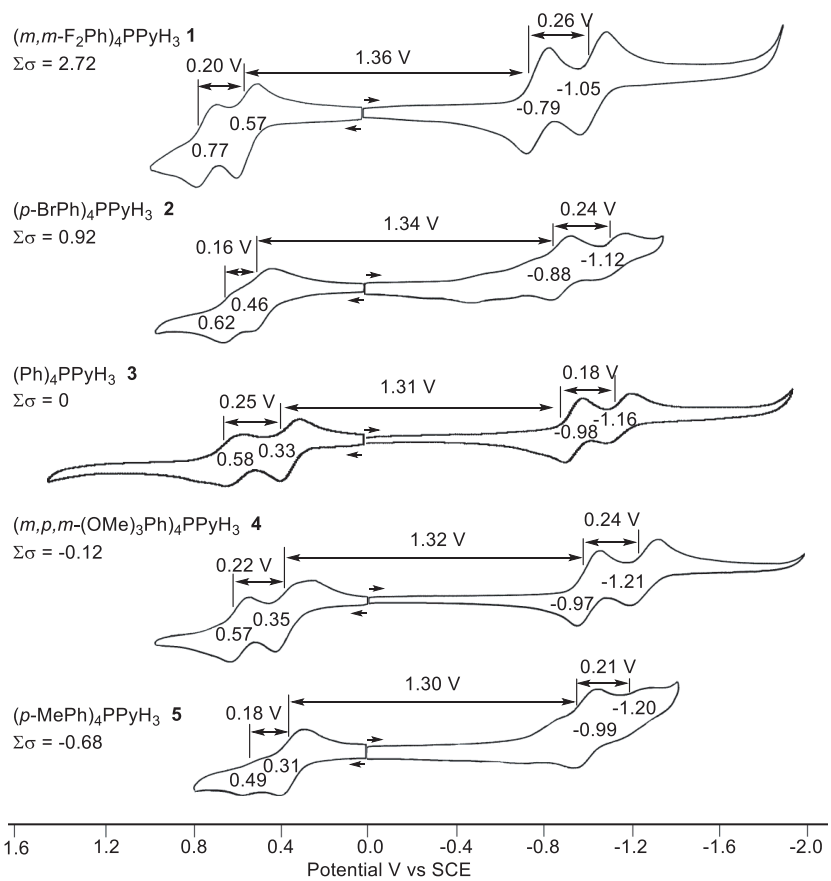

Fig. 2. Cyclic voltammograms of open-chain pentapyrroles **1–5** in CH_2Cl_2 containing 0.1 M TBAP

Table 2. Average potential differences between the first two oxidations (ΔE_{ox}), the first two reductions (ΔE_{red}) and the HOMO–LUMO gaps of compounds **1–5** in various solvents

Solvent	Ave. ΔE_{ox} (V)	ΔAve. ΔE_{red} (V)	Ave. HOMO–LUMO gap (V)
CH_2Cl_2	0.21 ± 0.04	0.23 ± 0.05	1.32 ± 0.04
PhCN	0.22 ± 0.03	0.29 ± 0.03	1.24 ± 0.03
Pyridine	0.33 ± 0.03	0.28 ± 0.03	1.09 ± 0.04

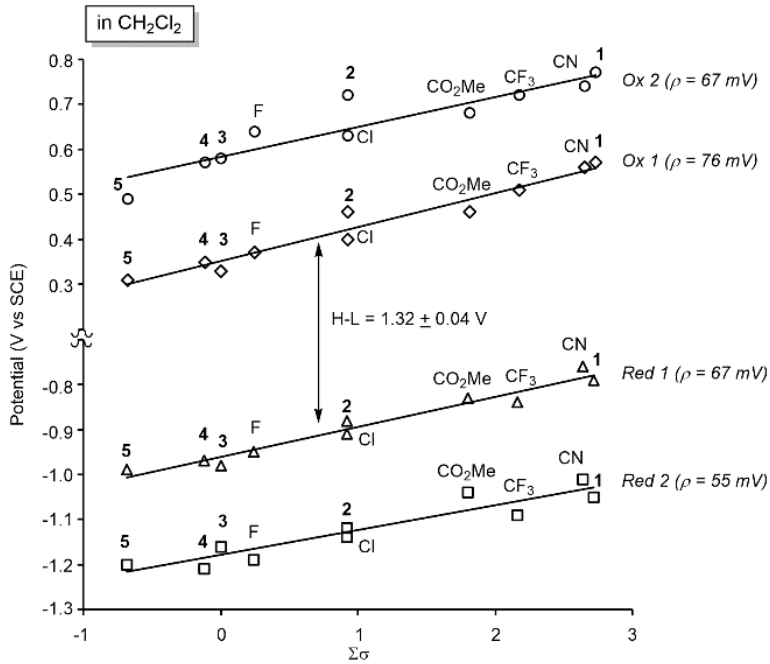

Fig. 3. Plots of half-wave potentials *vs.* the sum of Hammett substituent constants (Σσ) for open-chain pentapyrroles in CH_2Cl_2 containing 0.1 M TBAP

Table 3. Slopes of plots for $E_{1/2}$ *vs.* Σσ for the reversible redox reactions of open-chain pentapyrroles of the type $(Ar)_4PPyH_3$ and related free-base *meso*-aryl porphyrins $(Ar)_4PorH_2$ having similar *meso*-phenyl substituents

Compound	Solvent	ρ (mV)			
		Ox_1	Ox_2	Red1	Red2
$(Ar)_4PorH_2$[a]	CH_2Cl_2	65	—	73	64
$(Ar)_4PPyH_3$	CH_2Cl_2	76	67	67	55
	PhCN	61	57	65	67
	Pyridine	57	50	70	74[b]

[a]Data for porphyrins were taken from Ref. 14. [b]The ρ value was calculated without $(p\text{-MePh})_4PPyH_3$ **5**.

[5, 6, 8]. The values of ρ which were calculated in each solvent from $E_{1/2}$ *vs.* Σσ plots of the type shown in Fig. 3 are summarized in Table 3, which also includes data for structurally related free-base porphyrins possessing four substituted *meso*-phenyl groups **[14]**.

As shown in Table 3, the calculated ρ values for the two oxidations of the pentapyrrole are larger in CH_2Cl_2 (76 and 67 mV) than in PhCN (61 and 57 mV) or pyridine (57 and 50 mV) and an opposite trend is seen in pyridine, namely smaller effects of the substituents for oxidation than for reduction. However, the range of ρ values in Table 3 are similar to values observed for numerous porphyrins and corrole redox reactions of tetraaryl derivatives [15, 16] and this strongly suggests that there is not a significant difference in substituent effects between the electron-donating or electron-withdrawing groups on the four *meso*-phenyl rings of the open chain pentapyrroles and those on the four *meso*-phenyl rings of free-base tetraphenylporphyrin.

Protonation reaction

The open-chain pentapyrroles can add two protons in a single step as written in equation 2.

$$(Ar)_4PPyH_3 + 2H^+ \overset{\beta_2}{\rightleftharpoons} [(Ar)_4PPyH_5]^{2+} \qquad (2)$$

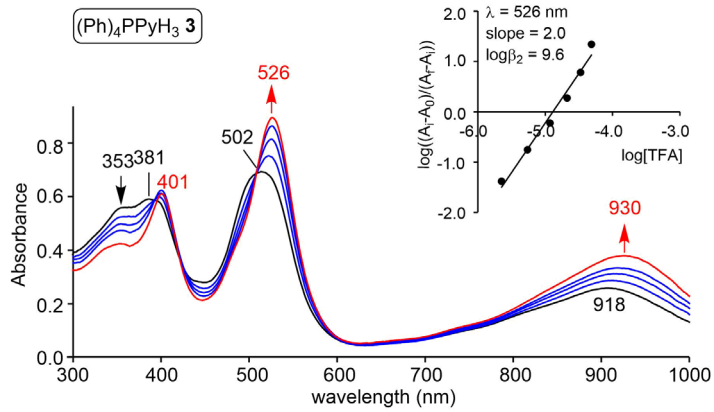

Fig. 4. UV-vis spectral changes of $(Ph)_4PPyH_3$ **3** during the protonation in CH_2Cl_2 with TFA. The Hill plot for the calculation of equilibrium constant is shown as inset

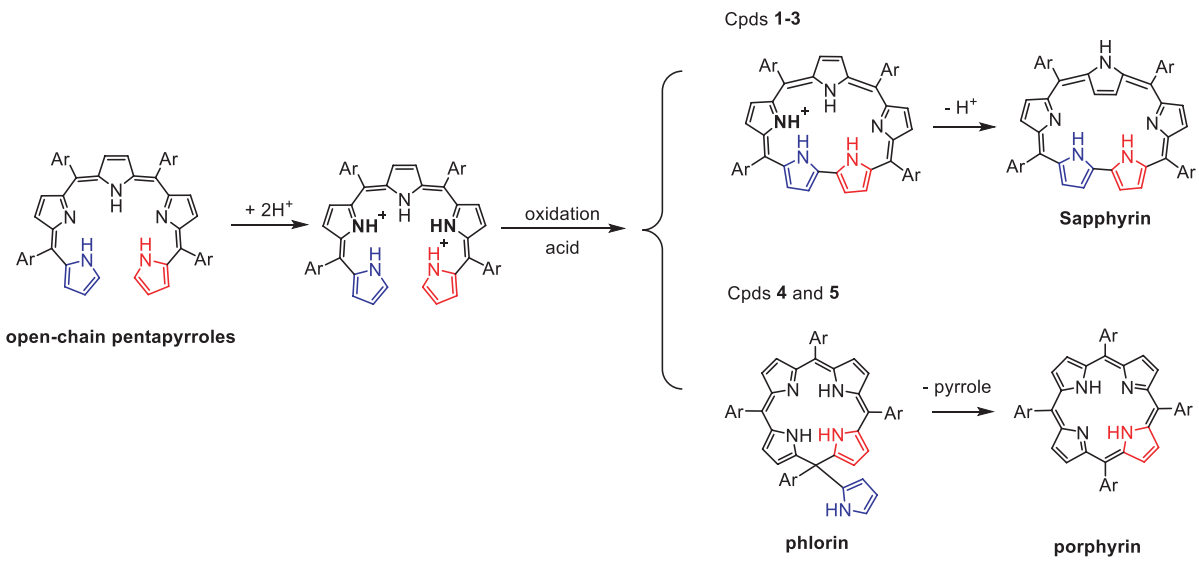

Scheme 1. Proposed overall mechanism for proton-induced oxidation reactions of open-chain pentapyrroles

An example of the spectral changes which occur during protonation of compound **3** is shown in Fig. 4 and the Hill plot used for calculating the equilibrium constant is given as an inset in the figure. The slope of the diagnostic plot is 2.0 which confirms a two-proton addition to the pyrrole nitrogens of this compound and the presence of well-defined isosbestic points in Figure 4 is consistent with the absence of intermediates during the conversion of $(Ph)_4PPyH_3$ to $[(Ph)_4PPyH_5]^{2+}$.

The same types of spectral changes and slopes of 2.0 were seen for all five newly synthesized pentapyrroles and a summary of the calculated equilibrium constants for these and previously characterized pentapyrroles is given in Table 4 where the measured $\log\beta_2$ ranges from 11.0 to 8.2, the exact value depending upon substituents on the phenyl rings which influences the basicity of the pyrrole nitrogens. Pentapyrroles with larger $\Sigma\sigma$ values have smaller $\log\beta_2$ values for the two-proton addition reaction. That is to say, the electron-withdrawing groups on the *meso*-phenyl rings make this protonation easier, a result which can be explained by the fact that the electron-withdrawing groups on the *meso*-phenyl rings pull electron density from the pyrrole nitrogens, thus making them less basic.

We anticipated that a linear relationship would exist between the measured $\log\beta_2$ and the $\Sigma\sigma$ for all of the pentapyrroles in Table 4 but this was not the case for all compounds (see Fig. S16), indicating that the basicity of the pyrrole nitrogens (and the measured $\log\beta_2$ values for protonation) were affected not only by the electron-donating or withdrawing properties of the *meso*-phenyl substituents but also by steric hindrance of these groups when it occurred [5].

The known proton-induced oxidation reaction to generate the closed-ring species [7, 8] was also studied for compounds **1–5**. Compounds **1–3** were partially converted to the closed-ring sapphyrin derivatives, but this was not the case for compounds **4** and **5** where no such conversion occurred. The proposed overall mechanism of this proton-induced reaction and side reaction is given in Scheme 1.

Table 4. UV-vis spectral data of $[(Ar)_4PPyH_5]^{2+}$ and equilibrium constants ($log\beta_2$) for protonation reactions of open-chain pentapyrroles containing different *meso*-substituents

X (Ar = XPh)	$\Sigma\sigma$[a]	λ/nm of $[(Ar)_4PPyH_5]^{2+}$			$log\beta_2$[b]	Ref.
m,*m*-F_2 **1**	2.72	404	529	899	8.5	*tw*
p-CN	2.64	411	534	918	8.2	[8]
p-CF_3	2.16	404	530	919	8.5	[8]
p-CO_2Me	1.80	411	536	935	9.1	[8]
p-Br **2**	0.92	407	505	894	9.0	*tw*
o,*p*-$(Cl)_2$	1.72	403	514	876	8.1	[5]
p-Cl	0.92	404	526	914	9.1	[5]
p-F	0.24	400	524	915	11.0	[5]
H **3**	0.0	401	526	930	9.6	*tw*
m,*p*,*m*-$(OMe)_3$ **4**	-0.12	391	535	944	9.8	*tw*
p-Me **5**	-0.68	403	488, 524	926	9.9	*tw*

[a]Values of σ were taken from Ref. [12]. [b]Values were calculated from the Hill plots. *tw* = this work.

According to previous studies, the *meso*-aryl pentapyrroles with electron-withdrawing groups on the *meso*-phenyl rings, especially those with steric-hindered moieties, can easily be oxidized in air after protonation and they then easily convert to mono-protonated sapphyrins under facile conditions [7, 8]. However, in the case of the pentapyrroles with electron-donating groups on the *meso*-phenyl rings, no sapphyrins seem to be generated from the open-chain compounds. Instead, porphyrin products are obtained after the oxidations [8]. An unexpected phlorin byproduct was detected by Ka and Lee during oxidation of a conjugated open-chain pentapyrrole [17] but, if formed, this phlorin could be easily converted under acidic conditions to a porphyrin product as observed in our earlier above-mentioned study.

X-ray crystal structure analysis

A plate-shaped crystal of compound **2** (*p*-BrPh)$_4$PPyH$_3$ was obtained and a single crystal X-ray diffraction experiment was carried out; the crystal structures are given in Fig. 5. As shown in Fig. 5a, the tetrabrominated molecule adopts a helix form which is maintained by intramolecular hydrogen bonds (N1–N2 = 2.716 (4) Å, N1–H···N2 = 123.7°, N3–N4 = 2.747 (4) Å, N3–H···N4 = 123.8°, N5–N4 = 2.793 (4) Å, N5–H···N4 = 123.9°). The centrosymmetric structure contains both helix form and right-and-left forms, which are present in the crystal packing. Some disordered chloroform solvents (18%/38%/44%) were found in the crystal structure and some geometric parameters of disordered components in each group were restrained by using EADP or SADI restraints. Additional details (X-Ray experimental data of compound **2** including Tables S3–S9) are given in the Supporting information and the cif files.

A comparison between the structure of the pentapyrrole (*p*-BrPh)$_4$PPyH$_3$ **2** described in the present work and a previously reported structure of (*p*-CF_3Ph)$_4$PPyH$_3$ [8] is given in Fig. 6. As seen in the figure, the cores of the two similar pentapyrroles (*e.g.* *p*-BrPh)$_4$PPyH$_3$ **2** (in red) and (*p*-CF_3Ph)$_4$PPyH$_3$ (in blue), are almost identical without the aromatic groups. A superposition of both helicoidal skeletons of these two molecules gives an RMSD of only 0.24 Å with a maximum deviation in the two pyrrole alpha carbon atoms being 0.53 Å, the main difference coming from the orientation of the aromatic substituents on the *meso*-positions of the molecule. This difference is due to the slight difference in the crystalline stacking and symmetry. Moreover, as seen in Fig. 6, the distance between the two α-carbons next to N1 and N5 is larger in the case of (*p*-BrPh)$_4$PPyH$_3$ **2** (6.22 Å in red) than in the case of (*p*-CF_3Ph)$_4$PPyH$_3$ (5.67 Å in blue).

Table 5 compares the X-ray structure of compound **2** with structures for three other pentapyrroles earlier

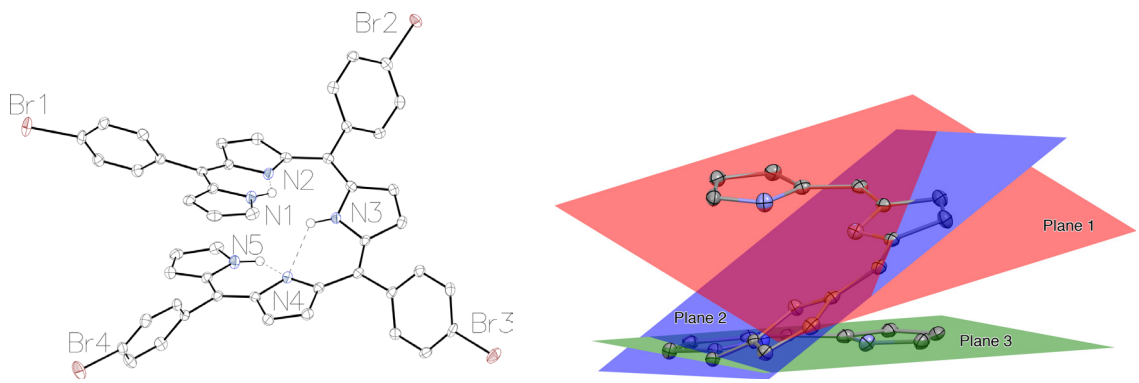

(a) (b)

Fig. 5. (a) ORTEP view of (*p*-BrPh)$_4$PPyH$_3$ **2**. Thermal ellipsoids plots are drawn at the 50% probability level. Disordered chloroform and H-atoms not involved in the H-bond are omitted for clarity. (b) View of centroid angle planes P1–P2–P3

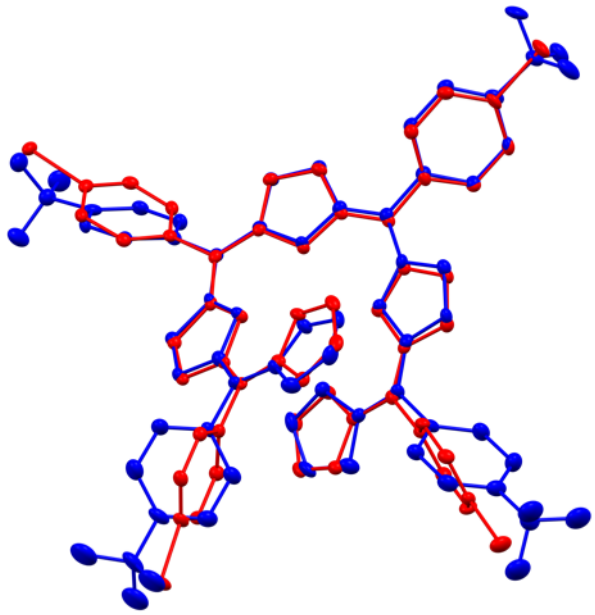

Fig. 6. Superimposition of the X-ray structure of $(p\text{-BrPh})_4PPyH_3$ **2** (in red) with previously reported structure of pentapyrrole $(p\text{-CF}_3\text{Ph})_4PPyH_3$ (in blue) [8]

reported in the literature [8, 18, 19]. The reference code in this table corresponds to the CCDC code. The torsion angle between the three planes, as defined in Fig. 5b, helps to evaluate the rolling-up and the hydrogen bonds. The number of intramolecular hydrogen bonds differs from one structure to another but has no obvious effect on the other structural parameters. The torsion angle between the P1–P2–P3 planes and the N1–N5 distance seems to be mainly determined by the nature of substituents at the β positions of the compound.

The N1–N5 distances, defined by the two nitrogen atoms located at the two extremities of the pentapyrroles, vary from 3.450 Å to 4.294 Å, the shortest distance being measured for the pentapyrrole-bearing methyl groups at the β-pyrrolic positions and without any aryl substituent groups at the *meso*-positions. The molecular configuration of the pentapyrrole can be tuned by the choice of the substituents at the *meso*-positions. By looking at the alpha-carbons (alpha C–C distances of each pyrrolic ring at the two extremities of the pentapyrrolic chain), we note that the $C_\alpha$pyrN1–$C_\alpha$pyrN5 distances vary from 5.007 A to 6.219 A, the longest distance being measured in case of compound **2**.

Table 5. Comparisons of four known open-chain pentapyrrole structures

Reference code	Compound 2	CUPBIZ (a)/(b) [15]	GATSUP 01 [16]	LEHNUK [8]
Structure	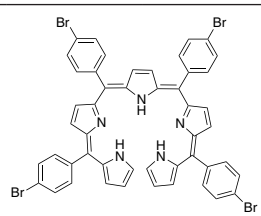	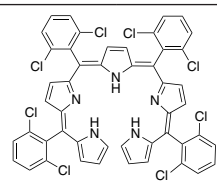	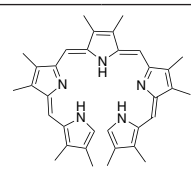	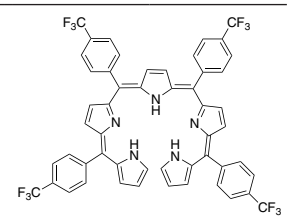
X-ray	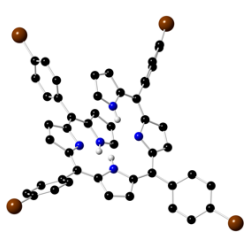			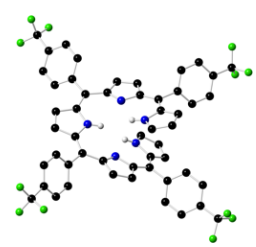
P1–P2–P3 (°)	43.1	47.8/47.5	43.2	42.0
N–H...N (Å) & angle (°)	2.718 123.7 2.747 123.8 2.793 123.9	2.361/2.213 123.2/123.2 2.211/2.126 120.5/120.8 2.256/2.543 123.4/135.9 2.364/2.514 126.9/127.1	2.148 126.0	2.238 122.2 2.240 121.6
H bonds	3	4	2	4
N1–N5 (Å)	4.294	3.787/3.781	3.450	3.628
$C_\alpha$pyrN1… $C_\alpha$pyrN5 (Å)	6.219	5.879/5.905	5.007	5.675
meso substituent	*p*-bromophenyl	*o,o′*-dichlorophenyl	none	*p*-trifluoromethylphenyl

CONCLUSIONS

The aryl substituents on the four *meso*-positions of the open-chain pentapyrroles can affect the electron transfer behavior of these pentapyrrolic species. At the same time, it will also change the basicity of the central pyrrole nitrogen. This may result from both the electronic structure (substituent effects) and the molecular configuration (steric effects), the latter of which requires further study in the future.

Acknowledgments

This work was supported by the Robert A. Welch Foundation (K.M.K., Grant E-680), the CNRS (UMR UB-CNRS 6302), the Université de Bourgogne Franche-Comté, the FEDER-FSE Bourgogne 2014/2020 (European Regional Development Fund) and the Conseil Régional de Bourgogne through the PARI II CDEA project and the JCE program. We are thankful to Mrs. Sandrine Pacquelet for technical assistance. ANR is granted for financial support (CO3SENS).

Supporting information

^{1}H NMR spectra, MALDI/TOF MS and HR-MS (MALDI/TOF) spectra, UV-vis spectra, cyclic voltammograms of compounds **1–5**, and CIF file giving crystallographic data for compound **2**, selected bond distances and angles as well as XYZ coordinates (DFT calculations) are given in the supplementary material. This material is available free of charge *via* the Internet at https://www.worldscientific.com/worldscinet/jpp. Crystallographic data have been deposited at the Cambridge Crystallographic Data Centre (CCDC) under number CCDC-1554869 for compound **2**. Copies can be obtained on request, free of charge, *via* http://www.ccdc.cam.ac.uk/data_request/cif or from the Cambridge Crystallographic Data Centre, 12 Union Road, Cambridge CB2 1EZ, UK (fax: +44 1223-336-033 or email: deposit@ccdc.cam.ac.uk).

REFERENCES

1. Gross Z, Galili N, Simkhovich L, Saltsman I, Botoshansky M, Blaeser D, Boese R and Goldberg I. *Org. Lett.* 1999; **1**: 599–602.
2. Simkhovich L, Rosenberg S and Gross Z. *Tetrahedron Lett.* 2001; **42**: 4929–4931.
3. Naumovski L, Sirisawad M, Lecane P, Chen J, Ramos J, Wang Z, Cortez C, Magda D, Thiemann P, Boswell G, Miles D, Cho Dong G, Sessler Jonathan L and Miller R. *Mol. Cancer Ther.* 2006; **5**: 2798–2805.
4. Koszarna B and Gryko DT. *J. Org. Chem.* 2006; **71**: 3707–3717.
5. Yuan M, Ou Z, Fang Y, Huang S, Xue Z, Lu G and Kadish KM. *Inorg. Chem.* 2013; **52**: 6664–6673.
6. Ou Z, Meng D, Yuan M, Huang W, Fang Y and Kadish KM. *J. Phys. Chem. B* 2013; **117**: 13646–13657.
7. Huang W, Ou Z, Chen X, Xue Z, Lu G, Wang H, Xiao J, Fang Y and Kadish KM. *J. Porphyrins Phthalocyanines* 2015; **19**: 794–802.
8. Shan W, Desbois N, Blondeau-Patissier V, Naitana ML, Quesneau V, Rousselin Y, Gros CP, Ou Z and Kadish KM. *Chem. — Eur. J.* 2017; **23**: 12833–12844.
9. Brault D and Rougee M. *Biochemistry* 1974; **13**: 4591–4597.
10. Dolomanov OV, Bourhis LJ, Gildea RJ, Howard JAK and Puschmann H. *J. Appl. Crystallogr.* 2009; **42**: 339–341.
11. Sheldrick GM. *Acta Crystallogr., Sect. C: Struct. Chem.* 2015; **71**: 3–8.
12. Zuman P. *Substituents Effects in Organic Polarography*. Plenum Press: New York, 1967.
13. Hansch C, Leo A and Taft RW. *Chem. Rev.* 1991; **91**: 165–195.
14. Kadish KM and Morrison MM. *J. Am. Chem. Soc.* 1976; **98**: 3326–3328.
15. Kadish KM, Van Caemelbecke E and Royal G. In *The Porphyrin Handbook*, Kadish KM, Smith KM and Guilard R. (Eds.). Academic Press: San Diego, 2000, Vol. 8, pp. 1–114.
16. Fang YY, Ou ZP and Kadish KM. *Chem Rev*. 2017; **117**: 3377–3419.
17. Ka J-W and Lee C-H. *Tetrahedron Lett.* 2001: 4527–4529.
18. Shin J-Y, Hepperle SS and Dolphin D. *Tetrahedron Lett.* 2009: 6909–6912.
19. Wagner UG, Kratky C, Falk H and Flödl H. *Monatshefte für Chemie* 1987; **118**: 1185–1194.